Environmental Science and Ecotechnology 28 (2025) 100633

Contents lists available at ScienceDirect

Environmental Science and Ecotechnology

journal homepage: www.journals.elsevier.com/environmental-science-and-ecotechnology/

Original Research

Utilizing network optimization to mitigate rising greenspace exposure inequalities in Chinese cities from 2000 to 2050

Rundong Feng [a,b,*], Bin Chen [b,c,**], Shenghe Liu [a], Fuyuan Wang [a], Kaiyong Wang [a], Bojie Fu [d]

[a] Institute of Geographic Sciences and Natural Resources Research, Chinese Academy of Sciences, Beijing, 100101, China
[b] Future Urbanity & Sustainable Environment (FUSE) Lab, Division of Landscape Architecture, Department of Architecture, Faculty of Architecture, The University of Hong Kong, Hong Kong SAR, 999077, China
[c] Urban Systems Institute, The University of Hong Kong, Hong Kong SAR, 999077, China
[d] Research Center for Eco-Environmental Sciences, Chinese Academy of Sciences, Beijing, 100083, China

ARTICLE INFO

Article history:
Received 11 April 2025
Received in revised form
7 November 2025
Accepted 7 November 2025

Keywords:
Greenspace exposure
Multi-scenario projections
Structural differences
Mitigate strategy
Network optimization

ABSTRACT

Urban greenspaces enhance human well-being and promote sustainable development in rapidly urbanizing regions by delivering vital ecosystem services, including cooling, air purification, and recreation. In China, where cities accommodate a large share of the population amid persistent environmental pressures, disparities in greenspace exposure pose a major obstacle to equitable access; these disparities arise from geographic, climatic, socioeconomic, and landscape factors. Although awareness of such inequalities is growing, their long-term trajectories, demographic and city-scale patterns, and viable spatial optimization approaches remain largely unexplored. Here we show that greenspace exposure inequality across 246 Chinese cities increased by 25% from 2000 to 2020 and is projected to rise further by 12.2–15.7% by 2050 under middle-of-the-road and fossil-fueled development scenarios, disproportionately affecting older, less-educated women and megacity residents. Geodetector and random forest analyses reveal that this rise results from interactions among greenspace coverage, population density, and patch connectivity, which explain 83.9% of the inequality. A network-based optimization approach that improves patch connectivity—without expanding total greenspace—can reduce disparities by 10.3–20.8%, with greater efficacy in high-inequality cities and among vulnerable populations. Our results highlight how precise landscape interventions can advance social equity in greenspace access, supporting Sustainable Development Goal 11 for inclusive, resilient urban environments.

1. Introduction

Urban areas currently accommodate more than half of the global population, with projections indicating an increase to 68% by 2050 [1]. However, climate change and environmental degradation threaten residents' well-being [2,3]. Greenspace is a crucial component of nature-based solutions [4,5] that provides multiple ecosystem services, such as cooling, air purification, and recreation [6–8]. Thus, the design and protection of greenspaces are effective strategies for achieving the United Nations Sustainable Development Goal 11 (SDG 11)—sustainable cities and communities [4,9]. However, achieving this goal through the provision of universal greenspaces remains a considerable challenge.

Greenspace provision (total or per capita) is the main indicator of greenspace accessibility [10–12]; in this context, the population-weighted exposure framework, which examines human–greenspace supply–demand relationships, has been widely adopted to assess greenspace exposure [4,13–15]. According to this framework, greenspace exposure improved in 1028 global cities from 2000 to 2018 [15], reducing associated inequality, particularly in the cities in the Global North, highly

* Corresponding author. Institute of Geographic Sciences and Natural Resources Research, Chinese Academy of Sciences, Beijing, 100101, China.
** Corresponding author. Future Urbanity & Sustainable Environment (FUSE) Lab, Division of Landscape Architecture, Department of Architecture, Faculty of Architecture, The University of Hong Kong, Hong Kong SAR, 999077, China.
E-mail addresses: fengrd.18s@igsnrr.ac.cn (R. Feng), binley.chen@hku.hk (B. Chen), liush@igsnrr.ac.cn (S. Liu), wangfy@igsnrr.ac.cn (F. Wang), wangky@igsnrr.ac.cn (K. Wang), bfu@rcees.ac.cn (B. Fu).

https://doi.org/10.1016/j.ese.2025.100633

urbanized areas [16], and developed countries [17]. Moreover, greenspace exposure inequality is mainly attributable to geography, climate, socio-economics, and greenspace landscape [14,15,18]. Specifically, geographic and climatic factors (e.g., temperature and precipitation) contribute to greenspace provision by influencing vegetation growth [18–20], socio-economic factors (e.g., population distribution and road construction) affect the allocation of greenspace resources through spatial planning and management [4,15], and greenspace landscape factors (e.g. connectivity and fragmentation) impact exposure inequalities by regulating the spatial form and structural configuration of greenspace patches [13,21,22]. However, differences in greenspace exposure inequalities between population groups and across city sizes remain unclear [23–25]. Therefore, there is an urgent need to assess structural differences in greenspace exposure inequalities and to propose forward-looking, differentiated measures to address the challenges of future climate and socio-economic change.

Spatial optimization strategies based on urban greenspaces are attracting increasing attention. Studies have found that increasing greenspace provision is an effective way to mitigate inequalities in human greenspace exposure [15,22] and facilitate several environmental benefits (e.g., cooling) [26,27]. However, increasing such provision within cities is difficult due to cost and spatial constraints [12,18,28]. Thus, effectively improving greenspace exposure in limited urban spaces through, for example, optimizing the patch connectivity within the spatial structure of greenspace networks, is crucial for urban planning [29,30]. Theoretically, protecting greenspace network cores involves the construction of multi-tiered ecological corridors that connect isolated greenspace patches and increase residential greenspace exposure by enhancing the linkage of these patches to their surroundings [31,32], ultimately reducing associated exposure inequalities [33]. Optimizing greenspace networks can also reduce the average distance residents travel to access greenspaces, thereby improving accessibility and reducing related inequalities [22,34]. In practice, increasing the connectivity of greenspace patches creates a more connected path network, mitigating exposure inequalities by improving residents' access to greenspaces [30,35], particularly in densely populated areas [34]. However, simulation studies integrating spatial constraints and network optimization are rare, leaving a gap surrounding in the climate-resilient development of greenspace planning for healthy cities [36].

To address this gap, this study combines multi-source data and methods to characterize the spatiotemporal changes in greenspace exposure inequality within Chinese cities under various shared socio-economic pathways and representative concentration pathways (SSP-RCPs) from 2000 to 2050, assessing differences across regions, demographics, and city sizes. It identifies the dominant factors of greenspace exposure inequality and proposes an optimization strategy to mitigate such inequality by enhancing the physical and spatial connectivity of the greenspace patches within network structures. Results provide forward-looking suggestions for more equitable urban greenspace planning, accelerating the realization of SDG 11's goal of making cities and human settlements inclusive, safe, resilient, and sustainable.

2. Materials and methods

2.1. Study area

This study selected 246 Chinese cities with urban areas larger than 90 km^2 in 2020. These cities encompassed 212 administrative units (including prefectural cities and municipalities) and 76.9% of China's population [22]. To identify contiguous areas of each city, the study used an urban area identification approach based on impervious surface distribution density [37] and urban clustering algorithms [38]; the applicability of this method was validated by related studies [6,39] (see Supplementary Text S1 for details). Thus, greenspace exposure was measured for the majority of the population in China's six geographic subregions [22,40]. The study further divided all cities into four groups according to their urban area: small cities (with urban sizes in the 0th–25th percentile), medium cities (25th–50th percentile), large cities (50th–75th percentile), and megacities (75th–100th percentile). The findings of this study can provide a reference for urban greening in other cities.

2.2. Data sources

The urban land cover data were based on projections of Chinese urban land cover [41] using four scenarios corresponding to the SSP-RCPs: sustainable (SSP1-2.6), middle of the road (SSP2-4.5), regional rivalry (SSP3-7.0), and fossil-fueled (SSP5-8.5) [42]. In this notation, the number following SSP represents different socio-economic pathways, and the number following RCP represents the future radiative forcing level versus the pre-industrial period. This dataset was developed by integrating the Global Change Analysis Model and the Future Land Use Simulation (FLUS) model [43] for land simulation with a 30 m resolution from the year 2000 to the year 2100 and includes eight urban land cover types (grassland, forest, shrub, water, cropland, barren, urban, and ice). This dataset offers two key advantages: (1) it can identify greenspace with higher spatial detail and greater historical accuracy (more than 1.7 times) than the previously commonly used 1 km resolution projection data [44,45] and (2) it considers the decline in demand for urban land based on future population decline to limit urban land growth [41,46]. In addition, this study used the latest 100 m Chinese population grid projection data and city-level population structure projection data under the SSPs [22]. The population grid projection data were built based on machine learning and showed good correlation with the historical data [47] (mean R^2 = 0.83, range: 0.80–0.86). The city-level demographic structure data were projected based on age, gender, and education using recursive multidimensional model and showed high accuracy with the validation of population census data [22]. The climate data were obtained from downscaled 1 km Coupled Model Intercomparison Project Phase 6 climate data from WorldClim (https://worldclim.org), and topography (elevation and slope), gross domestic product, and distance to urban areas and roads were obtained from the Resources and Environment Science and Data Center [6]. To ensure that the data covered the same temporal span, this study employed grid-scale analysis using bilinear spatial interpolation to resample relevant data to a 30 m resolution and administrative area-scale analysis (i.e., population structure inequalities) to aggregate relevant data to the administrative level.

2.3. Methods

The workflow of this study includes (1) assess the spatiotemporal dynamics of greenspace exposure and its inequality (Fig. 1a); (2) determine the dominant factors of greenspace exposure inequality (Fig. 1b); (3) identify the network of greenspaces (Fig. 1c); and (4) design a spatial optimization strategy using the FLUS model (Fig. 1d).

2.3.1. Greenspace exposure and inequality

In this study, forests, grassland, and shrubs were considered to be greenspace. To quantify greenspace exposure and its inequality, the study applied the population-weighted exposure model and

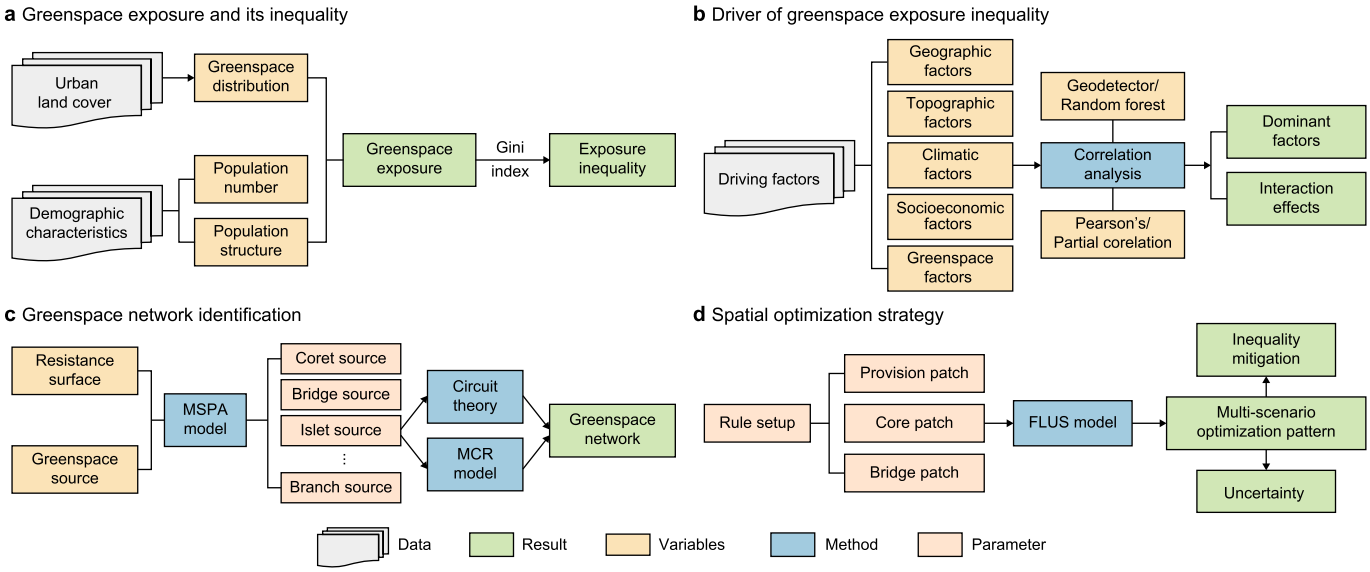

Fig. 1. Workflow of this study. **a**, Greenspace exposure and its inequality. **b**, Driver of greenspace exposure inequality. **c**, Greenspace network identification. **d**, Spatial optimization strategy. MSPA: Morphological spatial pattern analysis; MCR: Minimum cumulative resistance; FLUS model: Future Land Use Simulation model.

Gini index [4,14,15]:

$$G_d = \frac{\sum_{i=1}^{M} P_i \times E_{i,d}}{\sum_{i=1}^{M} P_i} \quad (1)$$

$$H = 1 - \frac{2 \times \sum_{i=1}^{n} \sum_{i=1}^{i} g_i}{n \times \sum_{i=1}^{n} gi} \quad (2)$$

where G_d is greenspace exposure with a buffer of d; P_i represents the population of grid i; and $E_{i,d}$ represents the greenspace coverage of grid i with a buffer of d, considering both central and nearby greenspace with a buffer of d. Previous studies found that 500 m was a reasonable range for greenspace exposure assessment [4,15], hence d is set 500 m. n is the total population, g_i is the magnitude of greenspace exposure for individual i (grid or city unit), and M is the total grid number. H represents the Gini index of greenspace exposure, ranging from 0 (absolute equality) to 1 (absolute inequality). A sensitivity analysis of greenspace exposure showed consistent results with different buffer distances (Supplementary Table S1).

To further estimate populations' greenspace exposure by age, sex, and education level, we first calculated the average greenspace exposure for each year from 2020 to 2050. Then, we estimated greenspace exposure inequality based on the urban population structure of the administrative units. We aggregated the data into five age groups (i.e., 0–19, 20–39, 40–59, 60–79, and >80 years), five education levels (i.e., illiterate, primary, secondary, bachelor, and master and above), and two sex groups (i.e., male and female). We also compared the historical results of greenspace exposure and inequality in 2020 with those in a related study [4], finding strong agreement ($R^2 > 0.8$, Supplementary Fig. S1).

2.3.2. Drivers of greenspace exposure inequality

We selected five categories of explanatory variables and examined their relationships with greenspace exposure inequality: (1) geographic (latitude and longitude); (2) topographic (elevation and slope); (3) climatic (mean annual precipitation and mean annual temperature); (4) socio-economic (proportion of population and urban land); and (5) greenspace landscape variables. Based on previous studies [4,18,48,49], we calculated five landscape variables for greenspace patches using the Fragstats software at a 30 m grid [50], where coverage rate represents composition, mean patch size and patch density represent fragmentation, and aggregation index and cohesion index represent connectedness (Supplementary Table S2). We rescaled all variables to a range of 0–1 using the maximum–minimum normalization method. Subsequently, we used Pearson's correlation coefficient (>0.3 and p value < 0.001) and partial correlation coefficient (>0.2 and p value < 0.001) for variable filtering. This study quantified the nonlinear relationship (q value) between the drivers and greenspace exposure inequality and the interaction contribution of the drivers using Geodetector [51,52] (Supplementary Text S2). Moreover, we performed the SHapley Additive exPlanations algorithm in the random forest [53] to verify the relationships between the variables and the Gini index of greenspace exposure. All data were randomly split into 80% and 20% for training and validation, respectively. Hyperparameters, including the number of trees to build, the number of features to use for splitting, the minimum leaf node size, and the maximum depth of the tree used, were tuned based on a grid search approach [54] (Supplementary Text S3).

2.3.3. Greenspace network identification

First, we used the morphological spatial pattern analysis model to extract greenspace patches with important implications for increasing connectivity and to identify greenspace network corridors for each city. Based on previous studies [55,56], a total of seven non-overlapping landscape features (i.e., core, bridge, islet, loop, edge, perforation, and branch) were identified using the eight-neighborhood analysis approach (Supplementary

Table S3). Second, based on circuit theory, we selected the core of greenspace patches in landscape connectivity as "sources" [55]. Resistance indicators and weights were established based on related studies [31,56], including nine elements (e.g., topography, land cover type, population, economic development, and infrastructure; Supplementary Table S4). Finally, the greenspace network and its buffer (consistent with greenspace exposure: 500 m) were identified using the minimum cumulative resistance model [57]:

$$C = f_{\min} \sum_{j=k}^{i=m} \left(D_{ij} \times R_i \right) \quad (3)$$

where C is the cumulative resistance of greenspace sources, $f_{\min}$ represents the minimum cumulative resistance, D_{ij} is the spatial distance from source grid i to source grid j, m and k represent the number of source grid i and j, respectively. R_i represents the resistance coefficient at grid i. Then, the ArcGIS software Linkage Mapper tool was applied to extract greenspace network corridors.

2.3.4. Network optimization strategy for greenspace exposure inequality

First, two rules were set for the network optimization strategy: (1) the "greenspace source" patches and the greenspace patches within the greenspace network and its buffer zones would not be transferred to other land classes during the land cover change, and (2) the total number of greenspaces in the target year (i.e., 2020 or 2050) would remain unchanged, with greenspace exposure inequality mitigated only by optimizing the urban landscape structure. The choice of these rules was mainly because (i) limitations in urban space prohibit a large increase in greenspace [22] and (ii) urban landscape optimization is more practicable and cost-effective than extensive greening for Chinese cities [32]. Therefore, greenspace network connectivity (measured by the cohesion index) can be used as a proxy for optimization in the context of constant greenspace provision [58].

Second, urban land cover was simulated using the FLUS model to implement the proposed network optimization strategy for each city. This model utilizes machine learning and cellular automation methods to effectively simulate urban land cover change processes [43,44]. We set up a transfer rule by increasing the transition costs of greenspace patches in the "Cost Matrix" module of the FLUS model and conducted sensitivity testing of the parameters (Supplementary Text S4). The simulated greenspace area for the target year remained constant, as predicted in the future urban land cover dataset [41] (i.e., no extra greenspace was introduced). To evaluate spatial uncertainty in the simulated results, we performed 1000 independent simulations to determine the probability of greenspace appearing at each location [58]. The effectiveness of the network optimization strategy is illustrated by comparing the resultant greenspace exposure inequalities with the original ones for the years 2020 and 2050. Finally, we selected Beijing and Hefei as typical cases for analysis. Since Beijing and Hefei are typical cities in the mid-to-late and early-to-mid stages of urbanization, respectively, they can provide targeted references for greenspace planning for cities at different development stages and offer effective practical information for related long-term spatial planning [41].

3. Results

3.1. Spatiotemporal patterns of greenspace exposure inequality

The results showed a rapid 25.2% increase in historical greenspace exposure inequality from 2000 to 2020 (Fig. 2a), especially in the north (55.5 ± 11.7%; mean ± standard deviation) and southeast (35.7 ± 10.0%) regions (Fig. 2b and c). The predicted paths substantially differed under different future scenarios. Under the regional rivalry and fossil-fueled scenarios, greenspace exposure inequality was expected to increase by 12.2% and 15.7%, respectively, with a more pronounced increase in the northeast region (>20%) (Fig. 2c). This result is completely opposite to that observed under the sustainable and middle of the road scenarios, which reduced greenspace exposure inequality (<10%), especially in the midcentral region (Fig. 2c). In addition, greenspace exposure inequality (1.1–1.8 times) and its change rate (1.2–2.7 times) were generally higher in the northeast, north, and northwest regions than in other regions (Supplementary Fig. S2). Under the sustainable scenario, more than 80% of cities showed decreases in exposure inequality, especially in the midcentral region (10.2 ± 5.4%). However, under the regional rivalry scenario, more than 70% of cities faced intensifying greenspace exposure inequality, especially in the north region (20.5 ± 8.3%).

3.2. Regional and structural differentiation of greenspace exposure inequality

This study found that, under the regional rivalry scenario, an additional 31.1 million people would be without exposure to greenspace by 2050 compared to 2020 (Fig. 3a). Under the fossil-fueled scenario, this number was estimated to be 18.2 million, located mainly in the northern and southeastern cities (>87%). Under the middle-of-the-road scenario, the population without exposure to greenspace decreased by 1.1 million. Under the sustainable scenario, this population decreased by more than 20.8 million, of which 41.4% were in the southeast region.

Structurally, greenspace exposure inequality tends to be higher among the elderly (age >60), females, and individuals with low education (illiterate and primary), as well as in megacities (Fig. 3b–d). Under the scenario scenarios, greenspace exposure inequality grew rapidly (>20%) among the elderly and in groups with low education levels (Fig. 3b and c); moreover, it was significantly greater for females than for males (two-sample t-test, p value < 0.01). Megacities exhibited the highest greenspace exposure inequality (Gini index >0.61) under the regional rivalry and fossil-fueled scenarios (Fig. 3d), though small- and medium-sized cities also exhibit large increases (>20%). Comparatively, under the sustainable scenario, there were fewer differences in Gini index values across sex, age, education level, and city size, and the greenspace exposure inequality for the elderly, the less-educated, and women, as well as for megacities, was reduced by an average of 26.7% (range: 23.8–30.1%).

3.3. Dominant factors in greenspace exposure inequality

Statistical analysis revealed that latitude in the geographic variable, precipitation in the climatic variable, population density in the socio-economic variable, and coverage and cohesion index in the greenspace landscape variable were significantly associated with the Gini index of greenspace exposure (Table 1). Moreover, population density ($q = 0.58 \pm 0.15$) and greenspace coverage ($q = 0.55 \pm 0.17$) primarily influenced greenspace exposure inequality, followed by cohesion index ($q = 0.54 \pm 0.12$), latitude ($q = 0.51 \pm 0.18$), and aggregation index ($q = 0.42 \pm 0.14$). The interaction analysis indicated that, together, coverage rate, population density, and cohesion index explained 83.9% of the Gini index of greenspace exposure, implying that greenspace supply, population demand, and patch connectivity interactively caused most greenspace exposure inequality. The random forest model

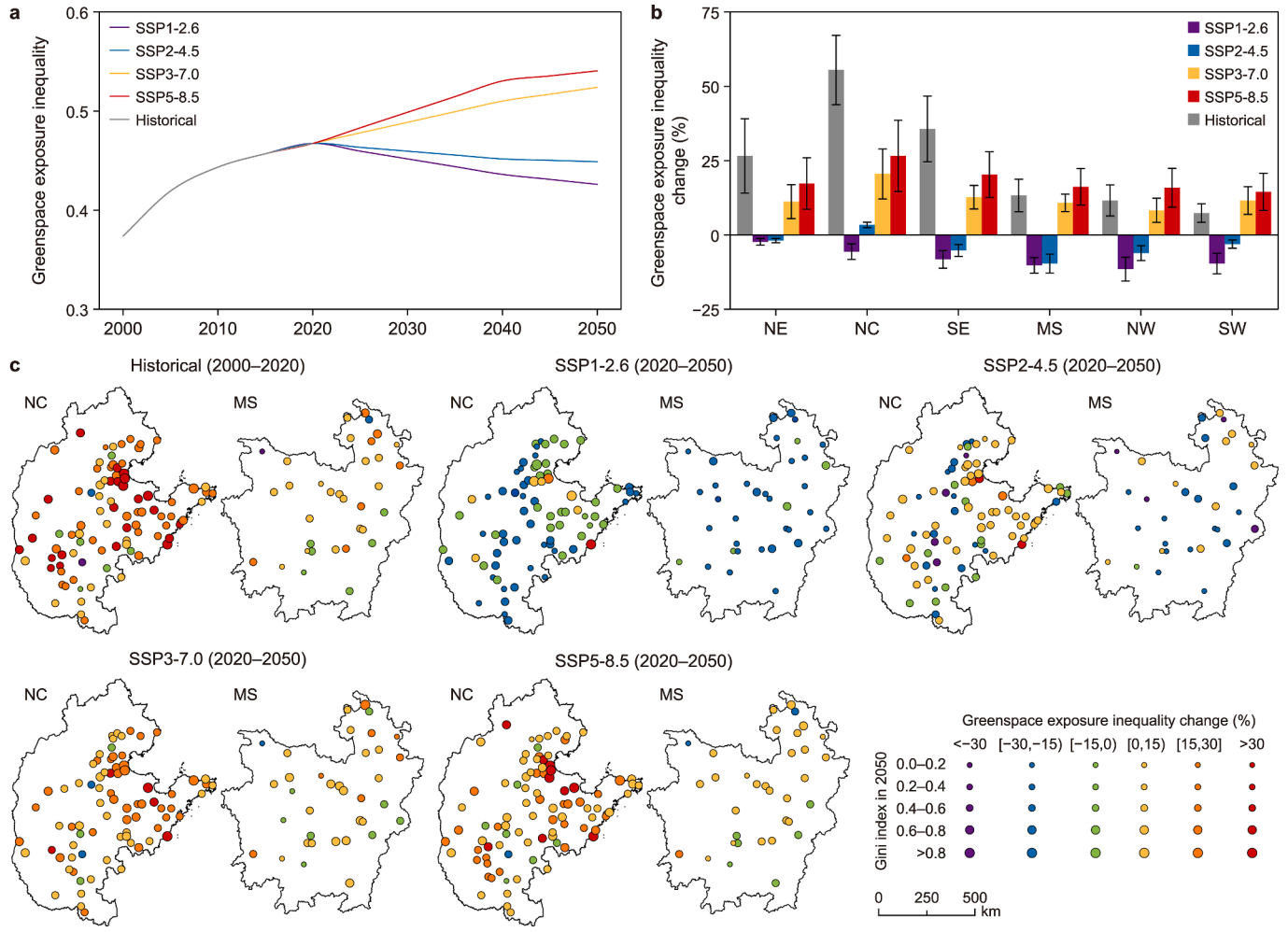

Fig. 2. Spatial-temporal patterns of greenspace exposure inequality measured by the Gini index. Temporal dynamic (**a**), regional differences (**b**), and region-level spatiotemporal changes (**c**) in greenspace exposure inequality. Larger bubble sizes represent higher Gini index values. NE: northeast region; NC: north region; SE: southeast region; MS: mid-central region; NW: northwest region; SW: southwest region. Error bars represent the 10th–90th percentiles.

results showed that the model explained over 85% of the variance (Supplementary Table S5), with coverage rate and cohesion index as important drivers. The importance of these two factors was higher under regional rivalry and fossil-fueled scenarios (Supplementary Fig. S3). Therefore, it is reasonable to optimize greenspace network connectivity (measured by the cohesion index) as a spatial strategy to mitigate inequalities in greenspace exposure.

3.4. Network optimization strategy for mitigating greenspace exposure inequality

Overall, the network optimization strategy proposed in this study could increase greenspace network connectivity by an average of 12.6–18.2%, while reducing the Gini index of greenspace exposure by an average of 10.3–20.8% (Fig. 4a). These percentages were higher in 2020 and under the regional rivalry and fossil-fueled scenarios. In particular, greenspace exposure inequality declined more sharply among women—especially older women (19.2 ± 6.1%) and women with lower educational levels (19.4 ± 8.2%)—and in megacities (20.7 ± 10.5%). Spatially, the network optimization strategy used in this study demonstrated a stronger potential for connectivity increase and greenspace exposure inequality mitigation in the northeast region (Supplementary Fig. S4), which was more evident under the regional rivalry and fossil-fueled scenarios (Fig. 4b). In contrast, the mitigation benefits in the midcentral region were lower (Fig. 4b), indicating that a network optimization strategy involving optimizing the greenspace network can effectively mitigate greenspace exposure inequalities through increasing patch connectivity, especially for particularly at-risk population groups and cities.

In practice, a detailed analysis of city-specific optimization strategy is needed; therefore, this study selected Hefei and Beijing as case cities to simulate the greenspace pattern and its spatial uncertainty (Fig. 5, Supplementary Fig. S5). The results revealed that our strategy can increase greenspace connectivity by an average of 12.9–20.6% in Hefei and 17.2–26.3% in Beijing and can mitigate greenspace exposure inequality by 13.1–25.3% and 18.7–31.7%, respectively (Supplementary Fig. S6a). The higher ends of these ranges occur in 2020 and under the regional rivalry and fossil-fueled scenarios. In addition, the cohesion index increases and stabilizes at 400 and 600 simulations for Hefei and Beijing (Supplementary Fig. S6b), respectively, indicating that the

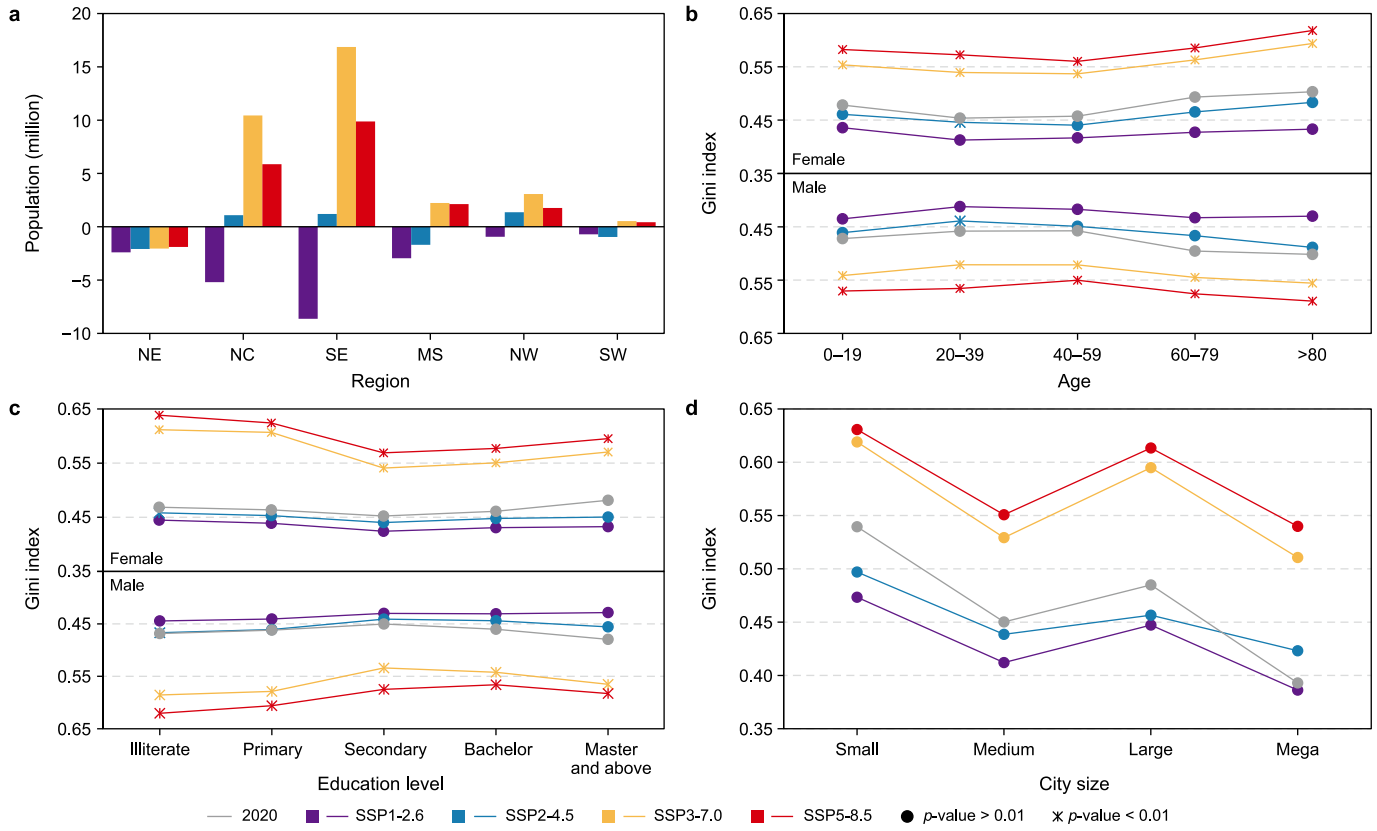

Fig. 3. Regional and structural differences in human exposure to greenspace under four SSP-RCPs scenarios. **a**, Population change without exposure to greenspace in different regions compared to 2020. **b**–**d**, Gini indices for greenspace exposure by age (**b**), education level (**c**), and city size (**d**). A two-sample *t*-test was used to compare males' and females' Gini index values for greenspace exposure. NW: northwest region; NE: northeast region; NC: north region; SE: southeast region; MS: midcentral region; SW: southwest region.

Table 1
Correlations (mean ± standard deviation) between explanatory variables and greenspace exposure inequality.

Category	Variable	Abbreviation	Correlation	Partial correlation	*q* value
Geographic	Latitude	Lat	0.46 ± 0.06****	0.26 ± 0.02****	0.51 ± 0.18****
	Longitude	Long	0.23 ± 0.03***	0.11 ± 0.01**	0.32 ± 0.14****
Topographic	Elevation	Elev	0.13 ± 0.02**	0.05 ± 0.01#	0.27 ± 0.10***
	Slope	Slope	0.05 ± 0.04#	0.01 ± 0.01#	0.15 ± 0.08**
Climatic	Mean temperature	Tem	−0.11 ± 0.02**	−0.05 ± 0.01#	0.26 ± 0.11****
	Mean precipitation	Prcp	−0.36 ± 0.04****	−0.24 ± 0.01****	0.3 ± 0.17****
Socio-economic	Urban land ratio	Const	0.41 ± 0.04****	0.17 ± 0.02	0.42 ± 0.13****
	Population density	Popd	0.52 ± 0.03****	0.28 ± 0.03****	0.58 ± 0.15****
Landscape	Mean patch size	MPS	−0.36 ± 0.06****	−0.15 ± 0.01**	0.37 ± 0.21****
	Patch density	PD	−0.22 ± 0.04*	−0.10 ± 0.01*	0.31 ± 0.16****
	Coverage rate	CR	−0.49 ± 0.05****	−0.27 ± 0.01****	0.55 ± 0.17****
	Aggregation index	AI	−0.35 ± 0.02***	−0.21 ± 0.01***	0.42 ± 0.14****
	Cohesion index	CI	−0.43 ± 0.05****	−0.24 ± 0.03****	0.54 ± 0.12****

Note: The partial correlation coefficient is derived by controlling for all other variables. ****, ***, **, *, and # indicate the proportions of *p* value < 0.001 for 100%, 75%, 50%, 25%, and 0%, respectively.

simulation results had reached their optimum value. Based on the rules and greenspace sources and network corridors (Fig. 5a–c), the simulation obtained the optimized greenspace exposure pattern in 2050 under the fossil-fueled scenario (Fig. 5b–d). Comparative results showed that the proposed strategy could increase greenspace exposure by an average of 180.3% in Hefei and 108.2% in Beijing, with results being more pronounced in the urban core and peripheral areas. Further, the strategy could reduce associated inequality from 0.46 and 0.61 in Hefei and Beijing to 0.37 and 0.45, respectively.

4. Discussion and implications

4.1. Discussion

As urbanization intensifies, greenspaces are receiving increasing attention due to their environmental, health, and socio-economic benefits [4,18,25,59]. China's urbanization has dramatically changed the way people access nature, resulting in greenspace exposure inequality [14,60,61]. However, the long-term trends of integrating historical and future human exposure to greenspaces are unclear, and sociodemographic differences pose analytical

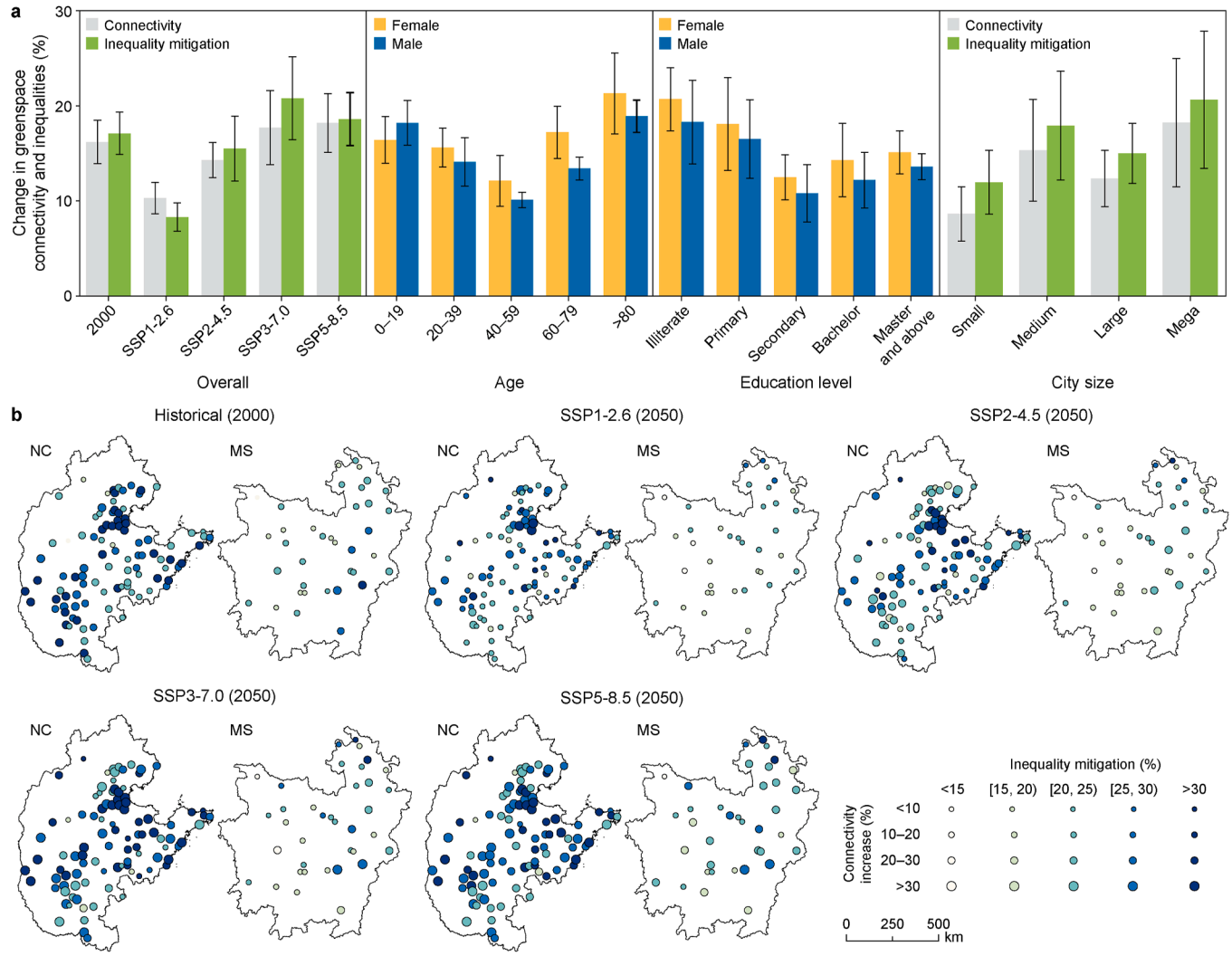

Fig. 4. Network optimization strategy for greenspace exposure inequality mitigation in 2020–2050. **a**, Mean change (%) of the connectivity (measured by the cohesion index) and inequality (measured by the Gini index) for greenspace by scenario, age, education level, and city size. **b**, Simulation patterns that achieve maximum mitigation in greenspace exposure inequality at the region level under four scenarios. Error bars represent the 10th–90th percentiles. NC: north region; MS: midcentral region.

challenges [4,13,62]. This study addresses these gaps by employing high-resolution future urban land cover and population data to predict the spatiotemporal changes in greenspace exposure inequality under various SSP-RCPs. By quantifying differences across regions, city sizes, and demographic characteristics, the study highlights the dependence of greenspace exposure inequality on the chosen development path. This study further proposes and validates a spatial mitigation strategy for greenspace exposure inequality in a specific, practical, and localized way. This strategy can provide policy support for the equitable use of greenspace resources across global cities. The findings reveal that appropriately increasing greenspace network connectivity can reduce greenspace exposure inequality by an average of 10.3–20.8%. This strategy is essential for achieving equal environmental sustainability within the constraints of urban spaces.

In contrast to previous studies [13,22], by integrating historical and future trends, this study found that inequalities in greenspace exposure were closely linked to urbanization pathways. During the historical phase (2000–2020), China's rapid urbanization and a large population influx encroached on substantial amounts of greenspace, resulting in a dramatic increase in greenspace exposure inequality [63,64]. During the future phase (2020–2050), results varied widely by scenario. Under the regional rivalry and fossil-fueled scenarios, greenspace exposure inequality would increase in more than 70% of cities due to the land overuse presumed in these scenarios [65,66], which significantly augmented exposure inequality (Fig. 2f and g). Conversely, the low population growth rates and environmentally friendly lifestyles of the sustainable scenario reduced the need for urban expansion [45,65]. Coupling these factors with advanced green technologies that could increase greenspace provision, this scenario reduced greenspace exposure inequality (Fig. 2a), thus emphasizing the critical role of addressing the interrelated social issues of development path, greenspace, and equity [42]. The north–south divergence in greenspace exposure and inequality was accentuated and even exacerbated in the regional rivalry and fossil-fueled scenarios. Low rainfall and low average temperatures limited the amount of greenspace and increased the costs associated with greenspace provision and maintenance, especially in the arid, rainless, and urban-planning-lagging cities in the northwest region [67,68]. Additionally, dense urban land patterns in urban planning encouraged the concentration of limited greenspace in certain communities, increasing the likelihood of unequal greenspace arrangements [13].

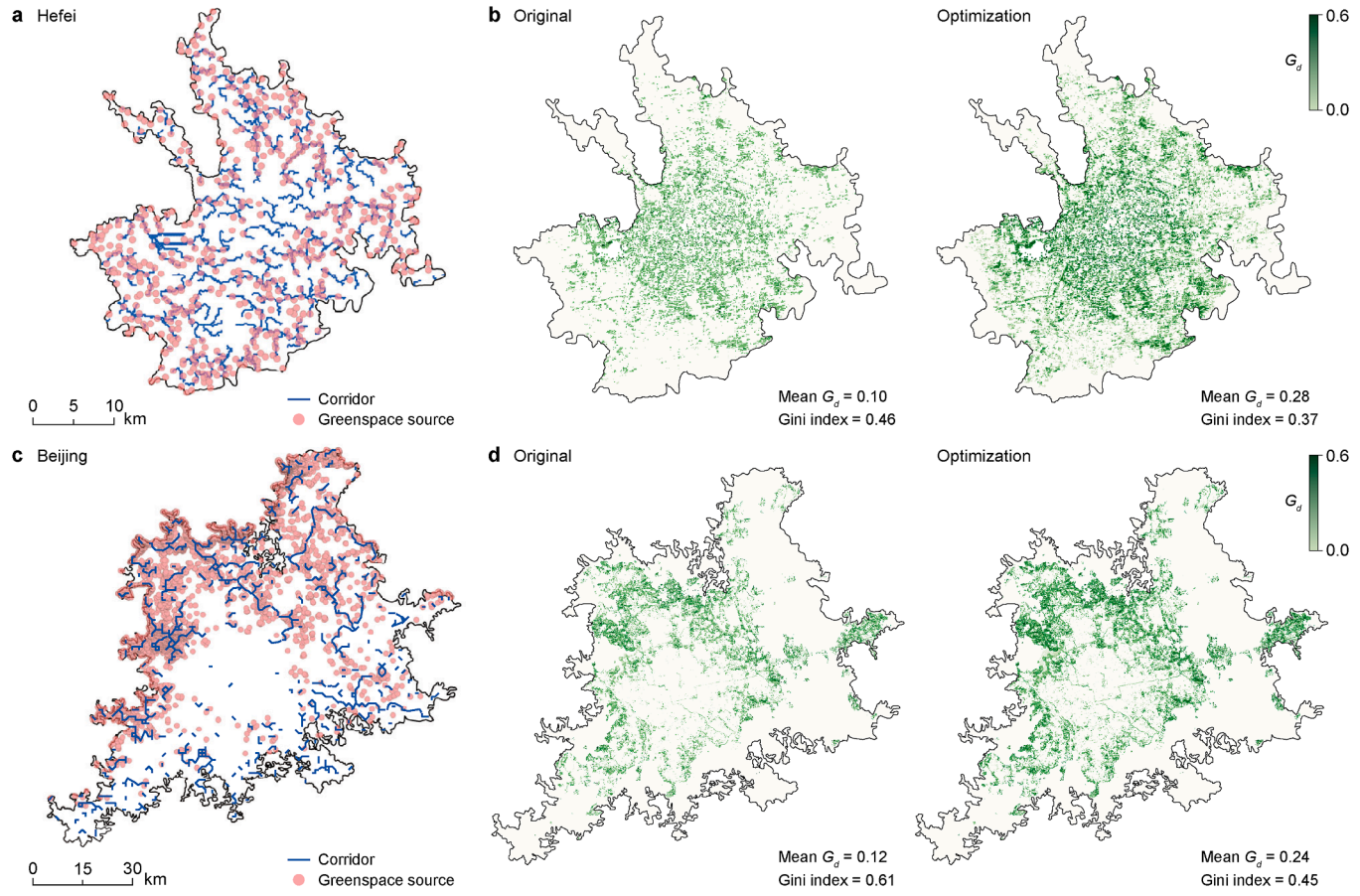

Fig. 5. Optimization strategy to mitigate greenspace exposure inequality in Hefei (**a**–**b**) and Beijing (**c**–**d**). **a**, **c**, Source and network corridors of greenspace. **b**, **d**, Original and optimization patterns of greenspace exposure (G_d) in 2050.

This study found that humans are unevenly exposed to greenspaces. In particular, older and less educated women and megacity residents will be threatened by greater inequalities. Under the fossil-fueled scenario, the elderly population in China was expected to reach half of the total population by 2050 (Supplementary Fig. S7), consistent with previous studies [47,69]. For this group, large reductions in greenspace will exacerbate exposure inequality. Low-income and low-education groups living in areas with inadequate infrastructure will yield a dearth of greenspace resources [13,64]; some women may lack awareness of or exhibit cultural preferences (e.g., physical activity habits) for ignoring the need for greenspace, resulting in a lack of initiative to visit greenspaces [4,22]. More importantly, urbanization, ageing (up to 36–50% in 2050 under four scenarios, Supplementary Fig. S7), and climate change amplify future public health risks, such as heat-related excess mortality, for these groups [70], while greenspace exposure inequality further exacerbates health inequities [41,59]. Additionally, megacities will face higher greenspace exposure inequality due to dense populations and inadequate greenspace provision, with housing market-driven residential segregation potentially exacerbating inequalities [7,60]. The sustainable scenario showed considerable potential for mitigating greenspace exposure inequality (Fig. 2c and 3a), providing a way forward for urban greening management. Therefore, understanding future multi-scenario trends in greenspace exposure in Chinese cities at fine temporal and spatial scales is important for designing long-term nature-based solutions to improve urban resilience to climate change and the protection of large at-risk populations.

4.2. Implications

Greenspace landscape, climatic conditions, and socio-economics are the main drivers of greenspace exposure inequality, consistent with previous findings [4,15]. Due to the limited availability of space within cities, direct and substantial increases in greenspace coverage can have enormous economic costs [12,18]. Our strategy offers new ideas for sharing equal greenspace resources. The modelling results showed that increasing the network connectivity of greenspace patches is an effective strategy for mitigating greenspace exposure inequality in urbanization, even without adding new greenspace (Figs. 3 and 4). For example, greenspace fragmentation due to urban expansion often occurs in densely populated areas [6,48]; thus, future urban planning could increase the spatial accessibility and connectivity of greenspace by building eco-corridors to connect different greenspace patches. Furthermore, improving the connectivity of greenspace patches (measured by the cohesion index) can reduce the distance travelled to greenspaces [4,22,49], strengthen ecosystem stability and urban resilience to climate risks [18,41,58], and ultimately improve greenspace accessibility and resident well-being [5]. Nevertheless, greenspace exposure inequality optimization strategy based on connectivity still faces potential implementation challenges, such as inadequate existing infrastructure, uneven resource allocation, and competing interests among multiple parties. Therefore, it is imperative to effectively address these concerns through stakeholder coordination, public participation, and technical support.

Specifically, for rapidly urbanizing cities, compact urban land use and renewal planning should be implemented to improve spatial accessibility and equity in greening by integrating greenspace functions (e.g., cooling, recreation, and sightseeing) and increasing patch connectivity through the introduction of small patches, depressions, rises, and other designs in large greenspaces. Our optimization strategy demonstrated strong mitigation potential in northern cities (Fig. 4b), effectively addressing this potentially salient problem. For highly urbanized cities, in addition to implementing sound planning and policy support for local conditions, it is crucial to consider the trade-offs and dynamic trends between the supply and demand and the spatial distribution of greenspace to promote a win-win situation in terms of environmental justice and urban efficiency. In addition, future greenspace planning should consider the demands of disadvantaged groups (e.g., the elderly, women, and people with low education levels) and different urbanization stages to develop more human-centered optimization strategies.

4.3. Limitations and perspectives

Some limitations and uncertainties should be acknowledged. First, multi-scenario analysis is beneficial for anticipating possible trends in greenspace exposure and developing forward-looking intervention strategies; however, this study was unable to capture the spatial details of greenspace exposure in the demographic structure. Since inconsistencies in the spatiotemporal resolution of some input data may lead to deviations in greenspace distribution simulations, further work should build a refined dataset with clear spatial information to improve simulation accuracy. In addition, future land cover and population projections cannot consider all relevant factors, such as greenspace allocation due to future extreme events and population control policies [22,41], thereby increasing the uncertainty of the analyses. Second, numerous landscape factors impact greenspace exposure inequality. Although this study selected commonly used and practical factors, additional factors should be included to strengthen the mitigation strategy. Moreover, although the population-weighted exposure model is a commonly used method of measuring greenspace exposure [4,13,14,21], exposure based on the buffer coverage metric cannot discriminate between physical accessibility (e.g., park entrances, opening hours) and greenspace quality (e.g., vegetation types, facility availability), which may lead to an overestimation of actual accessibility [14,63]. Therefore, future studies should explore the synergistic optimization of greenspace accessibility and quality (e.g., location, type, and safety) and use multi-agent simulation models (e.g., agent-based models) to improve analysis accuracy. Third, the Gini coefficient assumes equal utility of greenspace across different population groups and spaces [64], ignoring inter-group disparities and behavioral dimensions (e.g., visiting frequency or duration). To provide a more nuanced understanding of greenspace inequality, future work should apply additional indices (e.g., the Atkinson and Theil indices [15]) and incorporate them with accessibility analyses (e.g., based on OpenStreetMap road networks), points of interest, and spatialized population structure data.

5. Conclusion

Assessing multi-scenario trends and structural differences in greenspace exposure inequality, and proposing targeted, practicable mitigation strategies, are essential for urban adaptation and addressing climate change, thereby improving residents' well-being and promoting sustainable urban development. This study comprehensively assessed the evolutionary trends and structural differences of greenspace exposure inequality in China from 2000 to 2050. Under the regional rivalry and fossil-fueled scenarios, inequality in greenspace exposure is projected to be higher among older women with lower education levels and among residents of northern regions and megacities, whereas under the sustainable scenario, these disparities are substantially reduced. In addition, greenspace coverage, population density, and patch connectivity interactively accounted for 83.9% of greenspace exposure inequality. The study found that even without adding new greenspace, optimizing greenspace connectivity can reduce greenspace exposure inequality by 10.3–20.8% across four future scenarios, with the effect more pronounced in northern cities. Therefore, future urban greening should focus on optimizing urban landscape patterns to achieve universal greenspace availability for residents.

CRediT authorship contribution statement

Rundong Feng: Writing - Original Draft, Methodology, Formal Analysis, Conceptualization. **Bin Chen:** Writing - Review & Editing, Supervision, Methodology, Conceptualization. **Shenghe Liu:** Writing - Review & Editing, Supervision, Project Administration, Resources. **Fuyuan Wang:** Supervision, Project Administration, Funding Acquisition. **Kaiyong Wang:** Supervision, Funding Acquisition. **Bojie Fu:** Supervision.

Conflict of interest

The authors declare that they have no known competing financial interests or personal relationships that could have appeared to influence the work reported in this paper.

Acknowledgements

This study was supported by the National Natural Science Foundation of China (Grant Nos U24A20583, 42230510, 42271246, 42371253).

Appendix A. Supplementary data

Supplementary data to this article can be found online at https://doi.org/10.1016/j.ese.2025.100633.

References

[1] UN. United Nations, World urbanization prospects: the 2019 revision. https://population.un.org/wpp/, 2019.
[2] R.A. Garcia, M. Cabeza, C. Rahbek, M.B. Araújo, Multiple dimensions of climate change and their implications for biodiversity, Science. 344 (6183) (2014) 1247579.
[3] C. Hong, Q. Zhang, Y. Zhang, S.J. Davis, D. Tong, Y. Zheng, Z. Liu, D. Guan, K. He, H.J. Schellnhuber, Impacts of climate change on future air quality and human health in China, Proc. Natl. Acad. Sci. 116 (35) (2019) 17193–17200.
[4] B. Chen, S. Wu, Y. Song, C. Webster, B. Xu, P. Gong, Contrasting inequality in human exposure to greenspace between cities of Global North and Global South, Nat. Commun. 13 (1) (2022) 4636.
[5] S. Goodwin, M. Olazabal, A.J. Castro, U. Pascual, Global mapping of urban nature-based solutions for climate change adaptation, Nat. Sustain. 6 (4) (2023) 458–469.
[6] R. Feng, F. Wang, K. Wang, H. Wang, L. Li, Urban ecological land and natural-anthropogenic environment interactively drive surface urban heat island: an urban agglomeration-level study in China, Environ. Int. 157 (2021) 106857.
[7] R.F. Young, Managing municipal green space for ecosystem services, Urban For. Urban Green. 9 (4) (2010) 313–321.
[8] G. Lin, Y. Song, D. Xu, M.S.H. Swapan, P. Wu, W. Hou, Z. Xiao, Interpreting differences in access and accessibility to urban greenspace through geospatial analysis, Int. J. Appl. Earth Obs. Geoinf. 129 (2024) 103823.
[9] Z. Xu, J. Peng, Recognizing ecosystem service's contribution to SDGs: ecological foundation of sustainable development, Geogr. Sustain. 5 (4) (2024) 511–525.
[10] C. Huang, J. Yang, N. Clinton, L. Yu, H. Huang, I. Dronova, J. Jin, Mapping the

maximum extents of urban green spaces in 1039 cities using dense satellite images, Environ. Res. Lett. 16 (6) (2021) 064072.
[11] M. Bauwelinck, L. Casas, T.S. Nawrot, B. Nemery, S. Trabelsi, I. Thomas, R. Aerts, W. Lefebvre, C. Vanpoucke, A. Van Nieuwenhuyse, P. Deboosere, H. Vandenheede, Residing in urban areas with higher green space is associated with lower mortality risk: a census-based cohort study with ten years of follow-up, Environ. Int. 148 (2021) 106365.
[12] R.L. Rutt, N.M. Gulsrud, Green justice in the city: a new agenda for urban green space research in Europe, Urban For. Urban Green. 19 (2016) 123–127.
[13] Y. Song, B. Chen, H.C. Ho, M.-P. Kwan, D. Liu, F. Wang, J. Wang, J. Cai, X. Li, Y. Xu, Q. He, H. Wang, Q. Xu, Y. Song, Observed inequality in urban greenspace exposure in China, Environ. Int. 156 (2021) 106778.
[14] B. Chen, Y. Tu, S. Wu, Y. Song, Y. Jin, C. Webster, B. Xu, P. Gong, Beyond green environments: Multi-scale difference in human exposure to greenspace in China, Environ. Int. 166 (2022) 107348.
[15] S. Wu, B. Chen, C. Webster, B. Xu, P. Gong, Improved human greenspace exposure equality during 21st century urbanization, Nat. Commun. 14 (1) (2023) 6460.
[16] H. Wüstemann, D. Kalisch, J. Kolbe, Access to urban green space and environmental inequalities in Germany, Landsc. Urban Plann. 164 (2017) 124–131.
[17] E. Braae, S. Riesto, H. Steiner, A. Tietjen, European mass-housing welfare landscapes, Landsc. Res. 46 (4) (2021) 451–455.
[18] R.F. Hunter, M. Nieuwenhuijsen, C. Fabian, N. Murphy, K. O'Hara, E. Rappe, J. F. Sallis, E.V. Lambert, O.L.S. Duenas, T. Sugiyama, S. Kahlmeier, Advancing urban green and blue space contributions to public health, Lancet Public Health 8 (9) (2023) e735–e742.
[19] J. Xu, X. Liu, Q. Li, R. Goldblatt, W. Qin, F. Liu, C. Chu, Q. Luo, A. Ing, L. Guo, N. Liu, H. Liu, C. Huang, J. Cheng, M. Wang, Z. Geng, W. Zhu, B. Zhang, W. Liao, S. Qiu, H. Zhang, X. Xu, Y. Yu, B. Gao, T. Han, G. Cui, F. Chen, J. Xian, J. Li, J. Zhang, X.-N. Zuo, D. Wang, W. Shen, Y. Miao, F. Yuan, S. Lui, X. Zhang, K. Xu, L. Zhang, Z. Ye, T. Banaschewski, G.J. Barker, A.L.W. Bokde, H. Flor, A. Grigis, H. Garavan, P. Gowland, A. Heinz, R. Brühl, J.-L. Martinot, E. Artiges, F. Nees, D. P. Orfanos, H. Lemaitre, T. Paus, L. Poustka, L. Robinson, S. Hohmann, J. H. Fröhner, M.N. Smolka, H. Walter, R. Whelan, J. Winterer, K. Patrick, V. Calhoun, M.J. Li, M. Liang, P. Gong, E.D. Barker, N. Clinton, A. Marquand, L. Yu, C. Yu, G. Schumann, C. the, I. Consortia, Global urbanicity is associated with brain and behaviour in young people, Nat. Hum. Behav. 6 (2) (2022) 279–293.
[20] Y. Jin, Z. Yu, G. Yang, X. Yao, M. Hu, R.P. Remme, P.M. van Bodegom, J. Morpurgo, Y. Huang, J. Wang, S. Cui, Quantifying physiological health efficiency and benefit threshold of greenspace exposure in typical urban landscapes, Environ. Pollut. 362 (2024) 124726.
[21] Y. Song, B. Chen, M.-P. Kwan, How does urban expansion impact people's exposure to green environments? A comparative study of 290 Chinese cities, J. Clean. Prod. 246 (2020) 119018.
[22] R. Feng, B. Chen, S. Liu, F. Wang, K. Wang, R. Zhengchen, D. Wang, Future inequality of human exposure to greenspace resource and spatial utilization strategy in China, Resour. Conserv. Recycl. 218 (2025) 108231.
[23] M.J.A. Maes, M. Pirani, E.R. Booth, C. Shen, B. Milligan, K.E. Jones, M. B. Toledano, Benefit of woodland and other natural environments for adolescents' cognition and mental health, Nat. Sustain. 4 (10) (2021) 851–858.
[24] Y. Lu, L. Chen, X. Liu, Y. Yang, W.C. Sullivan, W. Xu, C. Webster, B. Jiang, Green spaces mitigate racial disparity of health: a higher ratio of green spaces indicates a lower racial disparity in SARS-CoV-2 infection rates in the USA, Environ. Int. 152 (2021) 106465.
[25] L.V. Pinto, C.S.S. Ferreira, P. Pereira, Temporal and spatial differences in human activities performed in urban green spaces of Vilnius (Lithuania), Geogr. Sustain. 5 (2) (2024) 302–317.
[26] Y. Li, J.-C. Svenning, W. Zhou, K. Zhu, J.F. Abrams, T.M. Lenton, W.J. Ripple, Z. Yu, S.N. Teng, R.R. Dunn, C. Xu, Green spaces provide substantial but unequal urban cooling globally, Nat. Commun. 15 (1) (2024) 7108.
[27] C. Xu, Q. Huang, D. Haase, Q. Dong, Y. Teng, M. Su, Z. Yang, Cooling effect of green spaces on urban heat island in a Chinese megacity: increasing coverage versus optimizing spatial distribution, Environ. Sci. Technol. 58 (13) (2024) 5811–5820.
[28] A. Russell, Z. Li, M. Wang, Equalizing urban agriculture access in Glasgow: a spatial optimization approach, Int. J. Appl. Earth Obs. Geoinf. 124 (2023) 103525.
[29] D. Caparros-Midwood, S. Barr, R. Dawson, Optimised spatial planning to meet long term urban sustainability objectives, Comput. Environ. Urban Syst. 54 (2015) 154–164.
[30] J. Guan, R. Wang, D. Van Berkel, Z. Liang, How spatial patterns affect urban green space equity at different equity levels: a Bayesian quantile regression approach, Landsc. Urban Plann. 233 (2023) 104709.
[31] K. Huang, L. Peng, X. Wang, W. Deng, Y. Liu, Incorporating circuit theory, complex networks, and carbon offsets into the multi-objective optimization of ecological networks: a case study on karst regions in China, J. Clean. Prod. 383 (2023) 135512.
[32] H. Liu, T. Niu, Q. Yu, L. Yang, J. Ma, S. Qiu, Evaluation of the spatiotemporal evolution of China's ecological spatial network function–structure and its pattern optimization, Remote Sens. 14 (2022).
[33] M. Rambhia, R. Volk, B. Rismanchi, S. Winter, F. Schultmann, Prioritizing urban green spaces in resource constrained scenarios, Res. Environ. Sustain. 16 (2024) 100150.
[34] E. Beele, R. Aerts, M. Reyniers, B. Somers, Spatial configuration of green space matters: associations between urban land cover and air temperature, Landsc. Urban Plann. 249 (2024) 105121.
[35] J. Chen, T. Kinoshita, H. Li, S. Luo, D. Su, Which green is more equitable? A study of urban green space equity based on morphological spatial patterns, Urban For. Urban Green. 91 (2024) 128178.
[36] K. Hu, S. Wang, F. Fei, J. Song, F. Chen, Q. Zhao, Y. Shen, J. Fu, Y. Zhang, J. Cheng, J. Zhong, X. Yang, J. Wu, Modifying temperature-related cardiovascular mortality through green-blue space exposure, Environ. Sci. Ecotechnol. 20 (2024) 100408.
[37] Q. He, R. Tan, Y. Gao, M. Zhang, P. Xie, Y. Liu, Modeling urban growth boundary based on the evaluation of the extension potential: a case study of Wuhan city in China, Habitat Int. 72 (2018) 57–65.
[38] H.D. Rozenfeld, D. Rybski, J.S. Andrade, M. Batty, H.E. Stanley, H.A. Makse, Laws of population growth, Proc. Natl. Acad. Sci. 105 (48) (2008) 18702–18707.
[39] Q. Meng, L. Zhang, Z. Sun, F. Meng, L. Wang, Y. Sun, Characterizing spatial and temporal trends of surface urban heat island effect in an urban main built-up area: a 12-year case study in Beijing, China, Rem. Sens. Environ. 204 (2018) 826–837.
[40] R. Feng, S. Liu, F. Wang, K. Wang, P. Gao, L. Xu, Quantifying the environmental synergistic effect of cooling-air purification-carbon sequestration from urban forest in China, J. Clean. Prod. 448 (2024) 141514.
[41] R. Feng, S. Liu, F. Wang, K. Wang, R. Zhengchen, D. Wang, Future urban ecological land transition and its implications for high-heat exposure in China, Sustain. Cities Soc. 111 (2024) 105590.
[42] B.C. O'Neill, E. Kriegler, K.L. Ebi, E. Kemp-Benedict, K. Riahi, D.S. Rothman, B. J. van Ruijven, D.P. van Vuuren, J. Birkmann, K. Kok, M. Levy, W. Solecki, The roads ahead: narratives for shared socioeconomic pathways describing world futures in the 21st century, Glob. Environ. Change 42 (2017) 169–180.
[43] X. Li, G. Chen, X. Liu, X. Liang, S. Wang, Y. Chen, F. Pei, X. Xu, A new global land-use and land-cover change product at a 1-km resolution for 2010 to 2100 based on human–environment interactions, Ann. Assoc. Am. Geogr. 107 (5) (2017) 1040–1059.
[44] W. Liao, X. Liu, X. Xu, G. Chen, X. Liang, H. Zhang, X. Li, Projections of land use changes under the plant functional type classification in different SSP-RCP scenarios in China, Sci. Bull. 65 (22) (2020) 1935–1947.
[45] N. Dong, L. You, W. Cai, G. Li, H. Lin, Land use projections in China under global socioeconomic and emission scenarios: utilizing a scenario-based land-use change assessment framework, Glob. Environ. Change 50 (2018) 164–177.
[46] G. Chen, X. Li, X. Liu, Y. Chen, X. Liang, J. Leng, X. Xu, W. Liao, Y.a. Qiu, Q. Wu, K. Huang, Global projections of future urban land expansion under shared socioeconomic pathways, Nat. Commun. 11 (1) (2020) 537.
[47] Y. Chen, F. Guo, J. Wang, W. Cai, C. Wang, K. Wang, Provincial and gridded population projection for China under shared socioeconomic pathways from 2010 to 2100, Sci. Data 7 (1) (2020) 83.
[48] R. Feng, F. Wang, K. Wang, Spatial-temporal patterns and influencing factors of ecological land degradation-restoration in Guangdong-Hong Kong-Macao Greater Bay Area, Sci. Total Environ. 794 (2021) 148671.
[49] F. Sharifi, I. Levin, W.M. Stone, A. Nygaard, Green space and subjective well-being in the Just City: a scoping review, Environ. Sci. Pol. 120 (2021) 118–126.
[50] K. McGarigal, S.A. Cushman, E. Ene, FRAGSTATS v4: Spatial Pattern Analysis Program for Categorical and Continuous Maps. in A. Computer Software Program Produced by the Authors at the University of Massachusetts, Computer software program produced by the authors at the University of Massachusetts, Amherst, 2012.
[51] J.-F. Wang, X.-H. Li, G. Christakos, Y.-L. Liao, T. Zhang, X. Gu, X.-Y. Zheng, Geographical detectors-based health risk assessment and its application in the neural tube defects study of the Heshun Region, China, Int. J. Geogr. Inf. Sci. 24 (1) (2010) 107–127.
[52] J.-F. Wang, T.-L. Zhang, B.-J. Fu, A measure of spatial stratified heterogeneity, Ecol. Indic. 67 (2016) 250–256.
[53] S.M. Lundberg, S.-I. Lee, A unified approach to interpreting model predictions, Adv. Neural Inf. Process. Syst. 30 (2017).
[54] B.W. Ang, H.C. Huang, A.R. Mu, Properties and linkages of some index decomposition analysis methods, Energy Policy 37 (11) (2009) 4624–4632.
[55] B. Wei, A. Kasimu, C. Fang, R. Reheman, X. Zhang, F. Han, Y. Zhao, Y. Aizizi, Establishing and optimizing the ecological security pattern of the urban agglomeration in arid regions of China, J. Clean. Prod. 427 (2023) 139301.
[56] E. Qiao, R. Reheman, Z. Zhou, S. Tao, Evaluation of landscape ecological security pattern via the "pattern-function-stability" framework in the Guanzhong Plain Urban Agglomeration of China, Ecol. Indic. 166 (2024) 112325.
[57] L. Li, R. Feng, G. Hou, J. Xi, P. Gao, X. Jiang, Integrating tourism supply-demand and environmental sensitivity into the tourism network identification of ecological functional zone, Ecol. Indic. 158 (2024) 111505.
[58] R. Feng, S. Liu, F. Wang, B. Chen, K. Wang, L. Xu, Current and future thermal effects and spatial optimization modelling of urban greenspace in megacity, Sustain. Cities Soc. 121 (2025) 106199.
[59] K.L. Ebi, K. Bowen, Green and blue spaces: crucial for healthy, sustainable urban futures, Lancet 401 (10376) (2023) 529–530.
[60] H. Yang, T. Chen, Z. Zeng, F. Mi, Does urban green space justly improve public health and well-being? A case study of Tianjin, a megacity in China, J. Clean. Prod. 380 (2022) 134920.

[61] S. Yang, W. Zhao, Y. Liu, F. Cherubini, B. Fu, P. Pereira, Prioritizing sustainable development goals and linking them to ecosystem services: a global expert's knowledge evaluation, Geogr. Sustain. 1 (4) (2020) 321–330.
[62] S. Wu, W. Yu, B. Chen, Observed inequality in thermal comfort exposure and its multifaceted associations with greenspace in United States cities, Landsc. Urban Plann. 233 (2023) 104701.
[63] Y. Lu, R. Chen, B. Chen, J. Wu, Inclusive green environment for all? An investigation of spatial access equity of urban green space and associated socioeconomic drivers in China, Landsc. Urban Plann. 241 (2024) 104926.
[64] A.J.F. Martin, T.M. Conway, Using the Gini Index to quantify urban green inequality: a systematic review and recommended reporting standards, Landsc. Urban Plann. 254 (2025) 105231.
[65] M.J. Gidden, K. Riahi, S.J. Smith, S. Fujimori, G. Luderer, E. Kriegler, D.P. van Vuuren, M. van den Berg, L. Feng, D. Klein, K. Calvin, J.C. Doelman, S. Frank, O. Fricko, M. Harmsen, T. Hasegawa, P. Havlik, J. Hilaire, R. Hoesly, J. Horing, A. Popp, E. Stehfest, K. Takahashi, Global emissions pathways under different socioeconomic scenarios for use in CMIP6: a dataset of harmonized emissions trajectories through the end of the century, Geosci. Model Dev. (GMD) 12 (4) (2019) 1443–1475.
[66] J. Gao, B.C. O'Neill, Mapping global urban land for the 21st century with data-driven simulations and Shared Socioeconomic Pathways, Nat. Commun. 11 (1) (2020) 2302.
[67] X. Wen, X. Deng, F. Zhang, Scale effects of vegetation restoration on soil and water conservation in a semi-arid region in China: resources conservation and sustainable management, Resour. Conserv. Recycl. 151 (2019) 104474.
[68] Y. Su, Q. Guo, H. Guan, T. Hu, S. Jin, Z. Wang, L. Liu, L. Jiang, K. Guo, Z. Xie, S. An, X. Chen, Z. Hao, Y. Hu, Y. Huang, M. Jiang, J. Li, Z. Li, X. Li, X. Li, C. Liang, R. Liu, Q. Liu, H. Ni, S. Peng, Z. Shen, Z. Tang, X. Tian, X. Wang, R. Wang, Y. Xie, X. Xu, X. Yang, Y. Yang, L. Yu, M. Yue, F. Zhang, J. Chen, K. Ma, Human-Climate coupled changes in vegetation community complexity of China since 1980s, Earths Future 10 (7) (2022) e2021EF002553.
[69] S. Zhang, M. Zhao, Z. Liu, F. Yang, B. Lu, Z. Zhao, K. Gu, S. Zhang, M. Lei, C. Zhang, C. Wang, W. Cai, City-level population projection for China under different pathways from 2010 to 2100, Sci. Data 10 (1) (2023) 809.
[70] J. Yang, M. Zhou, Z. Ren, M. Li, B. Wang, D.L. Liu, C.-Q. Ou, P. Yin, J. Sun, S. Tong, H. Wang, C. Zhang, J. Wang, Y. Guo, Q. Liu, Projecting heat-related excess mortality under climate change scenarios in China, Nat. Commun. 12 (1) (2021) 1039.